Rev.Adv.Mater.Sci. 10 (2005) 185-196

PROCESSING AND CHARACTERIZATION OF NANOCERAMIC COMPOSITES WITH INTERESTING STRUCTURAL AND FUNCTIONAL PROPERTIES

Guo-Dong Zhan[1,2] and Amiya K. Mukherjee[1]

[1]Department of Chemical Engineering & Materials Science, University of California, One Shields Avenue, Davis, CA 95616, USA

[2]now at University of Colorado, Chemical & Biological Engineering, 424 UCB, Boulder, CO 80309, USA

Received: May 08, 2005

Abstract. Nanocrystalline materials have demonstrated substantial changes in physical, chemical, and mechanical properties at severely diminished length scales. The extraordinary mechanical, electrical, and thermal properties of single-wall carbon nanotubes (SWCNTs), have prompted intense research into a wide range of applications in materials, electronics, chemical processing, and energy management. Attempts have been made to develop advanced engineering materials with improved or novel properties through the incorporation of carbon nanotubes in various matrices (polymers, metals, and ceramics). However, the potential application of carbon nanotubes in the reinforcement of ceramic composites has not yet been successfully demonstrated. Recently, we have successfully realized this possibility in reinforcing nanocrystalline ceramics through the use of a fast, comparably lower temperature, sintering technique e.g., Spark Plasma Sintering (SPS). SWCNTs were also successfully used to convert insulating nanoceramics to metallically conductive composites. Additionally, SWCNTs have been demonstrated as outstanding thermal barrier materials in ceramic systems for the first time. Novel thermoelectric properties have also been found recently in these nanocomposites. Such multifunctional carbon nanotube/ceramic composites are envisaged for a wide range of applications. These results will be discussed in the context of microstructural investigations and mechanistic interpretation. The current status and the challenges for the development of carbon nanotube composites are also outlined. In addition, recent findings on novel processing of transparent nanoceramic composites and new forming method for high-strain-rate and low-temperature superplasticity of nanocrystalline ceramic composites will be presented.

1. INTRODUCTION

Nanostructured materials is an exciting area of materials research because such bulk materials with grain size less than 100 nm exhibit novel properties as compared to their microcrystalline counterparts [1]. However, the brittleness of nanocrystalline ceramics has limited their potential and promise for use in structural and functional applications. Many strategies have been proposed to improve the mechanical properties of nanocrystalline ceramics by using reinforced second phases to develop nanometer-scale composite materials. Carbon nanotubes (CNT), originally discovered as a byproduct of fullerene research, are attracting increasing interest as constituents of novel nanostructured materials for a wide range of applications. There are many predictions for the potential applications of nanotubes, such as field emission displays, radiation sources, sensors, probes, interconnects, energy storage and conversion de-

Corresponding author: Amiya K. Mukherjee, e-mail: akmukherjee@ucdavis.edu

vices, hydrogen storage media, nanometer-sized semiconductor devices, and high-strength conductive composites. CNT should be ideal reinforcing fibers for composites. There are two main types of carbon nanotubes, single-wall carbon nanotubes (SWCNT) and multi-wall carbon nanotubes (MWCNT). Both of these types can have high structural perfection. SWCNT have a particularly desirable combination of mechanical, thermal, and electrical properties. Specifically, they have an elastic stiffness comparable to that of diamond (1.4 TPa), but they are several times as strong (yield strength 50 GPa). Moreover, carbon nanotubes conduct electricity along their length with very little resistance. Depending on bonding orientation within the nanotube, SWCNT may theoretically be either metallically conducting or semiconducting. The size, shape, and properties of SWCNT make them prime candidates for use in the development of potentially revolutionary composite materials.

The development of advanced engineering composites incorporating carbon nanotubes has become an interesting concept. Attempts have been made to develop advanced engineering materials with improved mechanical properties through the incorporation of CNT in various matrices (polymers, metals, and ceramics) [2-6] by taking advantage of the exceptional strength of the nanotubes. Most of the investigations on carbon nanotube containing composites have so far focused on polymer-based composites with improved electrical and mechanical properties. For example, their addition to a polymer matrix leads to a very low electrical percolation threshold and improved electrical conductivity. Work on carbon nanotubes in metals and ceramics has been much less focused. To date, the utilization of the extraordinary mechanical properties of carbon nanotubes in composites has not been successfully realized.

Additionally, theory predicts an extremely high value (6000 W/mK) for the room temperature thermal conductivity of an individual SWCNT, suggesting that SWCNT should be ideal for high-performance thermal management. Although this speculation has not yet been proven for SWCNT, a recent measurement of 3000 W/mK for the room temperature thermal conductivity of an *individual* MWCNT has been reported. However, the experimental measurements indicated that aligned bundles of SWCNT show a measured thermal conductivity of only 250 W/mK at room temperature and surprisingly, only 2.3 W/mK for the sintered sample. These results suggest that ropes of SWCNT would be ideal thermal barrier materials for thermal management application. However, no researcher has yet been concerned with thermal properties of carbon nanotube composites in ceramic systems. This study will report for the first time that ropes of SWCNT have been shown to successfully confer anisotropic thermal conductivity to nanoceramic materials.

Among nanostructures, carbon nanotubes have generated special interest due to their unusual properties, including both their thermal and electrical behavior. While the results of several investigations have been published, these have been directed to individual carbon nanotubes or to 'ropes', 'mats', and films of carbon nanotubes, in attempts to understand the thermoelectric properties and behavior of these materials. Typically, thermoelectric power of metallic carbon nanotubes is in the range of –50 ~ +65 μV/K at 300K. Greatly enhanced values (~ 260 μV/K) were discovered in semiconducting SWCNT devices. This opens up the possibility of using SWCNT for thermoelectric applications. Despite these investigations, an effective way to utilize carbon nanotubes in a thermoelectric application has been elusive since the high electrical conductivity and also high thermal conductivity of carbon nanotubes, the calculated ZT of pure CNTs can be expected to be very low (~10^{-4}). Recently, we discovered that incorporation of single-wall carbon nanotubes into nanoceramics leads to a dramatically improved electrical conductivity of the composites combined with a significant decrease in thermal conductivity, suggesting that the carbon nanotube reinforced nanoceramic composites might make promising thermoelectric materials [7-9].

Superplasticity can be defined as the ability of a polycrystalline material to undergo large elongations prior to failure. It can be described by the phenomenological equation,

$$\dot{\varepsilon} = \frac{A}{k_B T}\left(\frac{b}{d}\right)^{P}\left(\frac{\sigma}{E}\right)^{n} D_0 \exp\left(-\frac{Q}{k_B T}\right). \qquad (1)$$

In this equation, $\dot{\varepsilon}$ is the strain rate, A is a material constant, k_B is Boltzmann's constant, b is the Burgers vector, d is the grain size, σ is the applied stress, E is Young's modulus, D_0 is the pre-exponential factor for diffusion, Q is the activation energy for superplastic flow, and T is the temperature in degrees Kelvin. The constant n is the stress exponent, and p is the grain size exponent. The phenomenon usually occurs in fine-grained materials under conditions of moderate temperatures ($T > 0.5T_m$) and moderate-to-slow strain rates (10^{-6} to 10^{-2} s^{-1}). It is expected that nanocrystalline ceramics, which are characterized by a grain size in the

range of 10-100 nm, can deform at low temperatures and at high strain rates. However, evidence for really low temperature superplasticity in nanostructured materials is either very limited or not very convincing. To date, compressive superplasticity has been observed in several studies on nanocrystalline ceramics but elevated temperatures are required for this phenomenon to take place. In addition, the low superplastic strain rates (typically, 10^{-5}-10^{-4} s^{-1}) observed in fine-grained ceramics have limited their commercial applicability. Recently, high strain rate superplasticity (HSRS), which is usually referred to as the demonstration of high ductility at strain rates around 10^{-2} s^{-1}or greater, has stimulated much scientific and technological interest. The first HSRS report in ceramic materials is Kim *et al.* who reported a composite ceramic material with a submicron grain size that exhibits superplasticity at strain rates up to 1 s^{-1} at 1650 °C. Recently, we produced a nanocrystalline ceramic composite with the same composition and found that the deformation temperature can be reduced to 1400 °C. However, the prohibitively high deformation temperature makes it very difficult for commercial application. The realization of nanoceramic superplasticity into practice remains a challenging issue. In the present study we strive to bring the HSRS deformation temperature for nanoceramic composites down to 1050 °C or lower by using Spark-Plasma-Sintering (SPS) Apparatus, [10-12] both as a sintering tool as well as a forming tool.

2. EXPERIMENTAL PROCEDURE

The composites in this study were produced from consolidation of two types of alumina powders and SWCNT. The first type of powder was a mixture of α-alumina and γ-alumina, consisting of 80% α-Al_2O_3 and 20% γ-Al_2O_3 with particle sizes of 300 nm (40 nm crystallite size) and 20 nm respectively (Baikowski International Corporation, Charlotte, North Carolina). The second type was gas condensation synthesized γ-Al_2O_3 with average particle sizes of 15 nm and 32 nm (Nanophase Technologies Corporation, Austin, Texas, USA and Nanotechnologies Corporation, Darien, Illinois, respectively). Purified single-wall carbon nanotubes (SWCNT) in paper form, produced by the HiPco process with more than 90% of the catalyst particles removed were obtained from Carbon Nanotechnologies (Houston, Texas).

SWCNT tend to self-organize into 'ropes' that consist in many (typically, 10-100) tubes running together along their length in van der Waals bonding with one another. Due to their high surface area and high aspect ratio, the ability to homogeneously disperse the nanotubes into the matrix is a challenge in the processing. The SWCNT were received in the form of a pressed sheet or 'paper'. Care has been taken to mix the nanopowders and SWCNT. First, the as-received SWCNT in the 'paper' form must be dispersed into ethanol using an ultrasonic bath (40 Hz, ~50 °C, 2 hours, Branson Ultrasonic Cleaner B2510, American Airworks, Sophia, WV 25921). Second, alumina nanopowder was mixed with the dispersed SWCNT alcohol media. Finally, the composite powders were wet-sieved through 200-mesh, ball-milled for 24 h in ethanol using zirconia ball media, and then dried. Using these techniques three contents of SWCN at 5.7 vol.%, 10 vol.%, and 15 vol.% were produced. For certain experiments, the γ-Al_2O_3 nanopowder with particle size of 15 nm was mechanically activated by high-energy ball milling (HEBM) prior to being combined with the SWCNT. The high-energy ball milling was performed with 1 weight percent polyvinyl alcohol on a Spex 8000 mixer mill (Spex Industries, Metuchen, New Jersey, USA) in a zirconia vial. The polyvinyl alcohol was included to prevent severe agglomeration of the powder. Milling was performed at room temperature for 24 hours, after which time the polyvinyl alcohol was removed by heating the powder at 350 °C for 3 hours under vacuum. The alumina was then mixed with the SWCNT dispersion, and the combined dispersion was sieved, ball-milled, and dried as described above. An alumina-SWCNT mixture at 15% SWCNT, by volume, was prepared in this manner.

In order to obtain fully dense nanocomposites, retain nanocrystalline alumina grain size, and not damage the carbon nanotubes during sintering, spark plasma sintering (SPS) was employed in the present study. SPS is a moderate pressure sintering method based on the conjecture of a high temperature plasma momentarily generated in the gaps between powder materials by electrical discharge during DC pulsing. It has been suggested that the ON-OFF DC pulse energizing method could generate: (1) spark plasma, (2) spark impact pressure, (3) Joule heating, and (4) an electrical field diffusion effect. In this process, powders are loaded into a graphite die and were heated by passing an electric current through the assembly. The low heat capacity of the graphite die allows rapid heating. Therefore, SPS can rapidly consolidate powders to near theoretical density through the combined actions of a rapid heating rate, pressure application, and proposed powder surface cleaning. In our research,

spark plasma sintering is carried out under vacuum in a Dr. Sinter 1050 apparatus (Sumitomo Coal Mining Co., Japan). The powder mixtures were placed into a graphite die (20 mm in inner diameter) and cold-pressed at 200 MPa, giving rise to a sample size with a diameter of ~19 mm. Typical SPS processing parameters are: (1) an applied pressure between 50 and 100 MPa, (2) pulse cycles with a period of 2.5 ms and follow the pattern of 12 cycles on and 2 cycles off, and (3) maximum pulse parameters of 10,000 A and 10 V. After applying the given pressure, samples are heated to 600 °C in 2 minutes and then ramped to their sintering temperature at rates of 150 °C/min to 500 °C/min.

The final densities of the sintered compacts were determined by the Archimedes' method with deionized water as the immersion medium. The theoretical densities (TD) of the specimens were calculated according to the rule of mixtures. It is to be noted that the density of graphite (2.25 g/cm^3) was usually used for SWCNT but the estimated density for the present SWCNT is 1.8 g/cm^3. The density of carbon nanotubes is a function both of their diameter and number of shells. Microstructural observation was carried out using an FEI XL30-SFEG high-resolution scanning electron microscope (SEM) with a resolution better than 2 nm. Grain sizes were estimated from XRD and SEM images. Additional characterization by analytical electron microscopy and high-resolution transmission electron microscopy (HRTEM) was performed on a Philips CM-200 with a field emission gun operating at 200 kV. This instrument has a Link energy dispersive X-ray detector with energy resolution of 1.36 eV and a Gatan imaging filter with 1K by 1K CCD camera and energy resolution of 0.9 eV with 1nm spatial resolution. Indentation tests were performed on a Wilson Tukon hardness tester with a diamond Vickers indenter. The indentation parameters for fracture toughness (K_{IC}) measurements were a 2.5 Kg load with a dwell of 15s. The fracture toughness was calculated by using the Antis equation.

Electrical conductivity measurements using a four-wire-probe technique were carried out on an Agilent 34420A nano Volt/micro Ohm meter. Even at ambient temperatures, voltages can arise due to thermal EMF generated by dissimilar material junctions in the testing circuit. To remove the effect of these, or any other extraneous voltages, two readings are made for each measurement of conductivity: One reading is made with the current on and the other with the current off. The resulting change in voltage is used to calculate the conductivity of the specimens. Using this configuration, the meter has a resolution of 0.1 μΩ. The four-point probe electrical conductivity (σ) of the composites was measured at four temperatures –196 °C, -61 °C, 25 °C, and 77 °C.

Thermal diffusivity measurements were performed by the use of a Xenon Flash Thermal Diffusivity System both on the sintered disks and on rectangular bars cut from the sintered disks. The measurements were taken in two orientations, i.e., the orientation along the uniaxial compression axis, which is referred to herein as the 'transverse' orientation and the orientation perpendicular to the hot-pressing direction, which is referred to herein as the 'in-plane' direction. For each orientation, the measurement was performed by applying a short heat pulse (less than 1 millisecond in duration) to one surface of the disk or bar using a xenon flash lamp, while using an InSb infrared detector to measure the temperature change at the surface across from the surface to which the pulse was applied, the direction normal to the two surfaces defining the orientation being measured. Thermal conductivity is calculated from measurements of thermal diffusivity, specific heat, and bulk density. The room-temperature specific heat for alumina of 0.79 J/gK and ropes of SWCNT of 0.65 J/gK is used to calculate the thermal conductivity of the composites using the rule of mixtures.

Specimens for thermoelectric measurements were prepared by cutting the sintered compacts into rectangular bars whose dimensions were 14 mm × 5 mm × 1-3 mm. The heads of two Pt-Pt13%Rh thermocouples were embedded at the two ends, respectively, of each specimen and fixed with platinum wires. Thermoelectric properties of the specimens were then measured either in air or argon atmospheres by use of an automatic thermoelectric measuring apparatus (RZ2001K, Ozawa Scientific Co., Japan). Electrical conductivity measurements were performed at 300-900K by a DC four-probe technique.

3. RESULTS AND DISCUSSION

3.1. Processing and microstructure

In the open literature [2-3] all the other carbon nanotubes reinforced ceramic composites have been consolidated by hot-pressing methods that require higher temperatures and longer duration. These sintering parameters damage the carbon nanotubes in the composites, leading to decreases in, or total loss in, reinforcing effects and electrical conductivity. For example, in carbon nanotubes-metal-ceramic composite systems some of the hot-press-

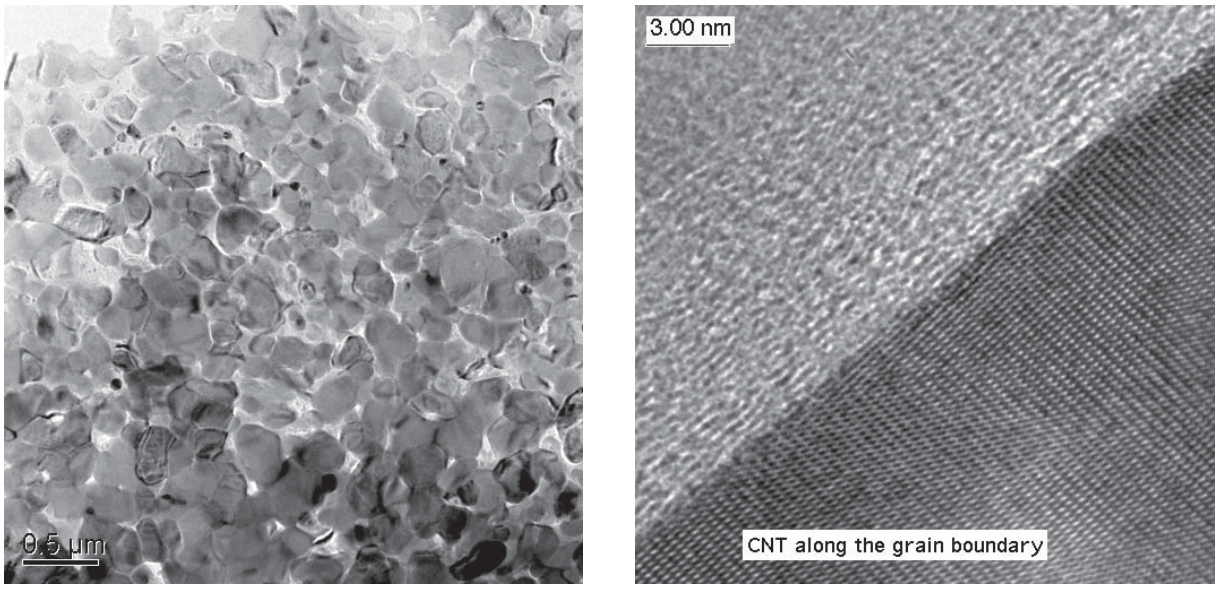

Fig. 1. TEM images of the nanocomposites showing the intertwining network structure of carbon nanotubes in the matrix. Fig. 1a is an image of the 10 vol.% SWCNT/Al_2O_3 composite. Light regions are filled with SWCNT bundles. Fig. 1b is a higher magnification image of the 10 vol.% SWCNT/ Al_2O_3 composite that shows the SWCNT concentrated at the boundaries between alumina grains.

ing temperatures were as high as 1600 °C. That damaged most of the carbon nanotubes and decreased the quantity and quality of carbon nanotubes in the sintered composites. Fully dense nanocomposites could still not be obtained. Siegel *et al.* [3] used the hot-pressing method at 1300 °C/ 1h to obtain fully dense multiple-wall carbon nanotubes filled alumina nanocomposites but the matrix grain size was in sub-micron range. Spark-plasma-sintering technique allows much lower sintering temperatures and shorter times for obtaining dense nanocrystalline ceramics as compared to conventional sintering techniques. It can be seen that the pure alumina nanopowders can be consolidated by SPS at 1150 °C for 180 seconds to get full density. The microstructure of the pure Al_2O_3 consisted of equiaxed grains with an average value of 350 nm. Note that both 5.7 vol.% SWCNT/Al_2O_3 and 10 vol.% SWCNT/Al_2O_3 nanocomposites can also be successfully consolidated to their theoretical densities at the same sintering conditions as that for pure alumina, suggesting that addition of SWCNT to the alumina matrix was not detrimental to the sintering process. The density of 10 vol.% SWCNT/Al_2O_3 nanocompo-site was decreased to 95.2% TD when the sintering duration time was shortened to two minutes at 1150 °C. Only 86% TD could be obtained when the sintering temperature was decreased to 1100 °C. These results show that spark plasma sintering is an effective sintering technique to obtain fully dense nanocrystalline ceramic composites without damaging carbon nanotubes. When γ-Al_2O_3 nanopow-ders were used, the sintering temperature to get dense materials is 50 °C higher than that for α-Al_2O_3 nanopowders. When high-energy ball milling was applied to the γ-Al_2O_3 nanopowders, the sintering conditions are the same as pure alumina while the obtained grain size is smaller than that for using α-Al_2O_3 nanopowders, suggesting the HEBM along with using finer alumina powders is beneficial to the consolidation process.

SEM and TEM analysis of the microstructures of the consolidated specimens was performed. Some interesting features can be noted. First, most of the alumina grains were less than 200 nm, indicating that the introduction of carbon nanotubes leads to refinement of grain size. When using much finer nanopowder such as γ-Al_2O_3 nanopowder and the use of HEBM processing technique, truly nanocrystalline grains less than 100 nm have been obtained. Second, it can be seen that carbon nanotubes are fairly homogenously dispersed in the matrix. A minor level of agglomeration was observed when the content of SWCNT was increased to 15 vol.%. Third, ropes of carbon nanotubes were effectively entangled with the alumina grains to form a network structure. These unique features observed in the present nanocomposites are quite different from *in-situ* carbon nanotubes reinforced alumina nanocomposites where the cohesion between carbon nanotubes and the matrix was rather poor and pullouts of carbon nanotubes were observed. Fig. 1a shows a typical

bright field TEM image of the 10 vol.% SWCNT/Al_2O_3 nanocomposite. This figure shows that ropes of single-wall carbon nanotubes are distributed along grain boundaries to develop an intertwining network microstructure. Some of catalyst particle such as iron were found in the ropes of carbon nanotubes. This microstructure simultaneously provides stiffness, toughness, and strength to the ceramic and also leads to continuity of the nanotube phase providing an interlinked electrical and thermal pathway for improved electrical conductivity and novel thermal properties. Good bonding between carbon nanotubes and alumina was observed in this material at HRTEM (Fig. 1b). XDS profile and spot scans were performed to analyze the chemical composition of the different grains, grain boundaries, and particles in the samples. The results showed that no other carbon forms such as graphite were detected along the grain boundary, suggesting carbon nanotubes were not damaged during the consolidation process by SPS.

3.2. Mechanical properties

Measured Vickers hardness and fracture toughness for pure alumina are 20.3 GPa and 3.3 $MPam^{1/2}$, respectively. Fracture toughness of 5.7 vol.% SWCNT/Al_2O_3 nanocomposite is over two times higher than that of pure alumina and there is almost no decrease in hardness. A toughness of nearly three times pure alumina was achieved in the 10 vol.% SWCNT/Al_2O_3 nanocomposite in the present study. No reinforcing effect was noted in the *in-situ* carbon nanotubes-Fe-Al_2O_3 nanocomposites in the investigation of Peigney *et al.* Moreover, only a marginal increase in fracture toughness can be obtained by improving the quality and quantity of carbon nanotubes in the latter work. The reasons given were mainly related to the damage of carbon nanotubes during hot-pressing. They also noted that volume contents of carbon nanotubes in the sintered products are lower than those in the starting powders. So far, the best reported result by Siegel *et al.* was a 24% increase in toughness in 10 vol.% MWCNT/Al_2O_3 nanocomposites. However, it can be seen that fracture toughness increases significantly with the introduction of single-wall carbon nanotubes for the present nanocomposites.

More interestingly it was found that there is a positive dependence of fracture toughness on the density in the 10 vol.% SWCNT/Al_2O_3 nanocomposites in addition to an increase of hardness with density. The dependence of hardness on density is reasonable, but the positive dependence of toughness is contrary to conventional expectation. This may be related to the extent of bonding of carbon nanotubes in the matrix as a function of density. As mentioned earlier, a network structure was developed in the fully dense nanocomposites where ropes of SWCNT were strongly entangled with alumina matrix. It can be noted that some of carbon nanotubes were entangled with alumina grains and some of them encapsulated alumina nano-scale grains. However, the situation is quite different for non-fully-dense nanocomposites. Depending on the density, SEM observation indicates that the entangling network structure appears to disappear in the 86%-TD nanocomposite where a loose network with a poor interfacial bonding can be noted. Stronger bonding of ropes with the matrix can be noted in the 95 %TD nanocomposite. These results suggest that the extent of interfacial bonding might be a factor in increasing the toughness of the composites.

Other toughening effects may be likely related to the following factors. First, it is due to extraordinary mechanical properties and the more perfect structure of SWCNT. MWCNT are similar to SWCNT, but contain more defects, which limit their properties. Furthermore, there are differences in the ability to transfer load from the matrix to the nanotubes between SWCNT and MWCNT. This may account for the improvement in the toughening effect between SWCNT in the present study and that observed in 10 vol.% MWCNT/Al_2O_3 [3]. Second, the toughening effect may be related to the unique entangling network structure. Therefore, crack deflection along the continuous interface between carbon nanotubes and nanocrystalline matrix grains is possibly one of the toughening mechanisms. Third, it is related to fast sintering technique that allows lower sintering temperatures and short duration. Therefore, the high quality ropes of single-wall carbon nanotubes can be retained in the sintered compacts. This is also consistent with the results by Flahaut *et al.* where the increase in the quality and quantity of SWCNT may result in an easier transfer of the stress and, thus, can account for the increase in the toughness in the in-situ SWCNT/Fe/Al_2O_3 nanocomposites. In order to be effective as reinforcing elements, high quality carbon nanotubes, without damage during consolidation, must be effectively bonded to the matrix so that they can actually carry the loads. The dependence of toughness on density directly supports this statement. Our present work gives a promising future for application of carbon nanotubes in reinforcing structural ceramic composites and other materials systems as well. Ongoing investigation to optimize the mi-

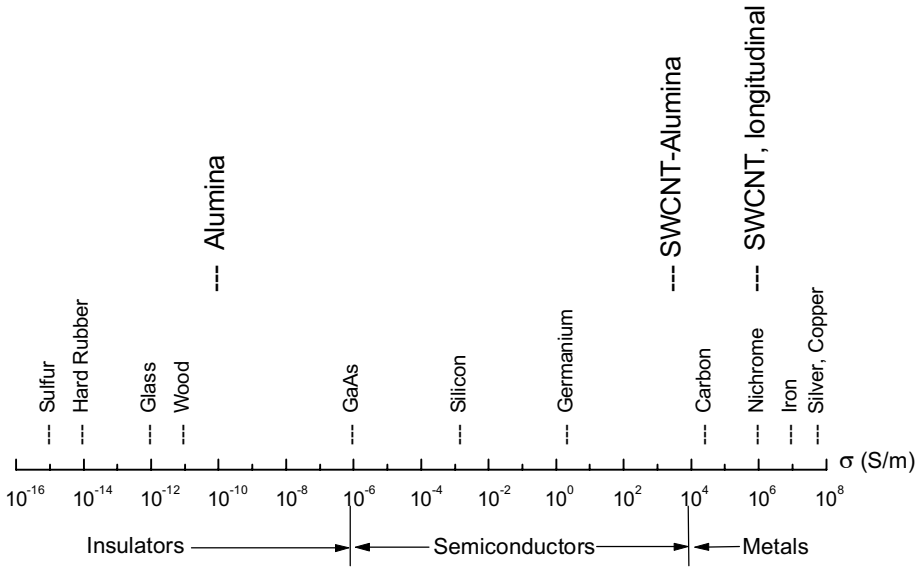

Fig. 2. The electrical conductivity of various representative materials at room temperature. Note the more than 13 orders of magnitude increase in conductivity of the 15 vol.% SWCNT-alumina composite compared to pure alumina.

crostructure and to examine the toughening mechanisms is currently underway.

3.3. Electrical properties

It is well known that pure alumina is an insulator with extremely low electrical conductivity (10^{-10}–10^{-12} S/m). It is interesting to note that the SWCNT/Al_2O_3 composites become much more electrically conductive when small amounts of carbon nanotubes were incorporated into alumina. It was found that the electrical conductivity increases with carbon nanotube content. The room-temperature electrical conductivity is up to 1050 S/m in 5.7 vol.% SWCNT/Al_2O_3 nanocomposite. More than three times the best reported conductivity of the CNT-Fe-Al_2O_3 nanocomposites (~ 400 S/m) has been obtained in our investigation in the 10 vol.% SWCNT/Al_2O_3 nanocomposite. An additional increase in conductivity (up to 3345 S/m) has been achieved in the 15 vol.% SWCNT/Al_2O_3 nanocomposite. This value is 735% higher than that of the hot-pressed CNT-Fe-Al_2O_3 nanocomposites. These values lie in the semiconductor range of conductivity but are very close to the metallic conductor threshold (10^4 S/m), as shown in Fig. 2. This dependence of the electrical conductivity on carbon nanotube content in the present ceramic nanocomposites is in contrast to the carbon nanotube metal matrix composites where the electrical conductivity decreases with carbon nanotube content.

The temperature dependence of the electrical conductivity of the alumina nanocomposites is shown in Fig. 3. The conductivity of the present nanocomposites increases with increasing temperature. The largest conductivity increase, from 2060 S/m at –194 °C to 3375 S/m at 77 °C, is in the 15 vol.% SWCNT/Al_2O_3 nanocomposite. This behavior is also opposite to the trend in metal matrix composites containing carbon nanotubes. It has also been reported that carbon nanotube-metal-oxide

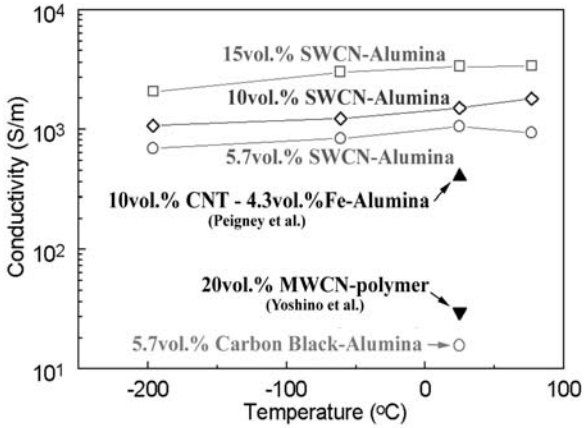

Fig. 3. The temperature dependence of the electrical conductivity of alumina nanocomposites.

nanocomposites can be aligned to improve the electrical conductivity by high temperature extrusion. The best reported conductivity measured along the extrusion direction is 2000 S/m whereas much lower values are measured in the transverse direction (~ 60 S/m) in CNT-Fe/Co-$MgAl_2O_4$ systems. Note that the best conductivity in the aligned $MgAl_2O_4$-based systems could only be obtained in the center of the extrusion while other regions were quite low due to the damage of the nanotubes by exposure to high-temperature extrusion.

The significant increase in electrical conductivity may be related to the use of high-quality ropes of SWCNT that were distributed along grain boundaries to develop an intertwining network of electrically conducting pathways. In order to directly compare the effects of the network structure an additional composite was produced. The experimental procedure and materials were identical to the 5.7 vol.% SWCNT/Al_2O_3 composite except carbon black was substituted for the SWCNT. The carbon black is composed of mixed fullerenes and has an average particle size of 42 nm. The 5.7 vol.% carbon black/ Al_2O_3 composite had a measured conductivity of 15 S/m, nearly two orders of magnitude less than the corresponding SWCNT containing composite.

3.4. Thermal properties

Fig. 4 is a bar graph showing the thermal diffusivities of various samples. The first three sets of bars each represent measurements taken directly on sintered disks in the transverse direction, while the last two sets represent measurements in transverse and in-plane directions taken on bars cut from sintered disks. It is very interesting to note that the incorporation of ropes of SWCNT does not change the in-plane thermal diffusivity of the matrix. By contrast, the transverse thermal diffusivities are significantly decreased when the carbon nanotubes are present, and that an increase in the level of carbon nanotubes produces a greater drop in thermal diffusivity in the transverse direction. These findings are directly in contrast to the results observed for SWCNT/polymer composites.

The temperature dependence of the transverse thermal diffusivity for pure alumina and composites has been measured in the temperature ranges from 25 to 500 °C. The thermal diffusivity of the pure alumina and carbon nanotube composites decreases with increasing temperature. This is consistent with the results observed for other carbon materials. Moreover, it is interesting to note that the transverse thermal diffusivity of 15 vol.% SWCNT/Al_2O_3 composite increases slightly from room temperature to ~100 °C and then decreases with increasing temperature until 300 °C. Above that the curve coincides with that of 10 vol.%SWCNT composite. The observed reduction in thermal diffusivity with increasing temperature can be attributed to the dominant effect of Umklapp scattering (phonon-phonon scattering) in reducing phonon mean-free path length.

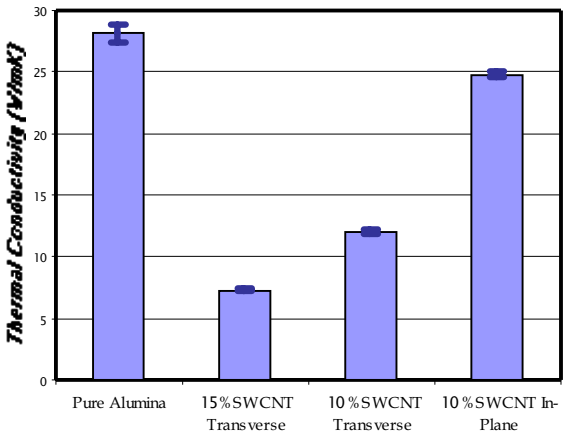

Fig. 4. Bar graph comparing thermal diffusitivites of various materials in different materials and orientations.

3.5. Thermoelectric properties

The thermopower measurement of the 10 vol.% SWCNT/20 vol.% 3Y-TZP/Al_2O_3 composite was carried out in air atmosphere. It was found that thermoelectric power (Seebeck coefficient) increases linearly with increasing temperature. The measured values are ranging from 28.5 μV/K at 345K to 50.4 μV/K at 644K. The lowest temperature data is comparable to that of aligned ropes of SWCNT (~27 μV/K at 300K). The positive value of thermopower is consistent with the oxygen-doping p-type semiconducting behavior of SWCNT. It can be seen (Fig. 5) that the electrical conductivity of the composite decreases with increasing temperature, indicating the metallic conducting behavior. It was found that the residual catalyst remaining in the SWCNT plays a critical role in the charge and thermal transport of the composites. This is different from that of purified SWCNT/ceramic composites. Also, the electrical conductivity of the composite is extremely low, which is more than two orders of magnitude lower than that of purified SWCNT/ceramic composites. Previous studies found that the in-plane thermal conductivity of the CNT/ceramic composites depends on that of the matrix and it decreases with

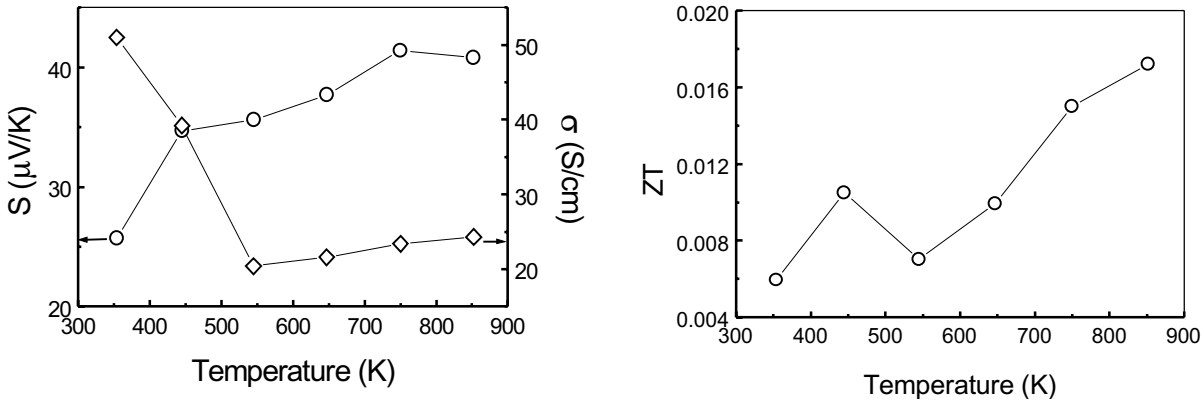

Fig. 5. Variable-temperature charge transport and thermal transport data for 10 vol.%SWCNT/3Y-TZP nanocomposite: (a) Thermopower (*S*) and electrical conductivity (σ) and (b) thermoelectric figure of merit, *ZT*, as a function of temperature. Thermal conductivity of 0.2 W/mK was used for the calculation of *ZT*. This is referred to the data for SWCNT/YSZ composites in the temperature range of 27-1100 °C. The measurement was carried out in argon atmosphere.

increasing temperatures. It has been reported that incorporation of SWCNT into zirconia leads to the development of the lowest thermal conductivity of the composites. The measured thermal conductivity of the composites was in the range of 0.2-0.4 W/mK in the temperature range of 27-1100 °C [9]. It was found that the present 10 vol.% SWCNT/3Y-TZP composite has the highest electrical conductivity among all the composites. It is interesting to note that the electrical conductivity decreases with increasing temperature until 545K and then increases slowly with increasing temperature above that value. The thermopower also has a positive sign and it increases with increasing temperature. Based on this data, the calculated *ZT* of the composite is shown in Fig. 5. It was found that the ZT increases with increasing temperature and has a value of 0.018 at 850K. This is two orders of magnitude higher than that of pure SWCNT. As compared to other thermoelectric materials, however, the electrical conductivity of the CNT/ceramic composites is low. This can be further improved if pure metallic SWCNT can be utilized due to the much higher electrical conductivity of SWCNTs.

3.6. Ultra-Low-Temperature superplasticity

SPS has been demonstrated not only to be an effective sintering process to fabricate fully dense nanocrystalline ceramics and composites but also to be a new forming method to enhance ceramic ductility [9,10]. The first attempt to apply the SPS approach to speed up superplastic forming was by Shen *et al.* who started with fully dense ceramics that sinter via either transient or permanent liquid phase modes. The observed enhanced ductility is thought to be associated with the enhanced grain sliding at the boundary of the glassy/liquid phase resulting from the electric-field induced motion of charged species. Despite remarkable success (rapid superplastic deformation with high strain rates in the range 10^{-2} to 10^{-3} s^{-1}), the deformation temperatures were still extremely high (1500 °C is typical). In the present study, completely different strategies and ideas were utilized. Here we started with a porous preform instead of fully dense blanks and *simultaneously* consolidated and superplastically formed the specimens in the SPS equipment. The use of concurrent deformation and consolidation provides nanoceramic superplasticity with many advantages. First, porous preforms are easy to produce (75-90% TD) by different methods such as pressureless sintering, plasma spray, SPS, etc. Second, in term of effects of pore pinning, the presence of open porosity network in the materials at densities below 90% TD was found to seriously inhibit static grain growth during the sintering. However, at densities over 90% TD density, as the open pores become closed, the closed pores are not as effective as open pores in pinning grain boundaries, and thus beyond this point the grain size begins to increase dramatically. It has been found that the open porosity can also limit dynamic grain growth during the deformation. Finally, the microstructure with nanocrystalline grain size can lead to much

lower deformation temperatures and higher strain rates.

The starting materials used in the present study include high purity alumina powder doped with 500-ppm MgO and 300-ppm Y_2O_3 obtained from Baikowski International and cubic MgO nanopowder with a particle size of 40 nm. 86.7 wt.% Alumina and 13.3 wt.% MgO were mixed by conventional ball-milling method with ethanol alcohol and zirconia balls in a plastic vessel for 24 hours to prepare a composite powder. The composite mixture was consolidated by SPS to produce a composite consisting of 50 vol.%Al_2O_3 and 50 vol.%$MgAl_2O_4$ (through the solid reaction of Al_2O_3 and MgO during sintering). SPS was carried out under vacuum in a Dr. Sinter 1050 SPS apparatus (Sumitomo Coal Mining Co., Japan) with pulse duration of 3.3 ms. The pulse sequence consists of twelve pulses followed by two periods (6.6 ms) of zero current. The temperature was monitored with a thermocouple inserted into a 'non-through' hole (2 mm in diameter and 5 mm in depth) in the graphite die. The sample was a disk shape with a diameter of ~20 mm and a thickness up to 4 mm. The compressive deformation tests of SPS-prepared, partially dense nanoceramic composites were performed via the same SPS apparatus. Before the desired temperature was reached, a constant load of about 3-4 kN was applied to the sample, which corresponds to an initial stress of 40-50 MPa. When the desired temperature was reached, constant load rates of 45-125 N/s were applied. The compressive strain is defined here as $Ln\ (1\text{-}\Delta L/L_0)$, where ΔL and L_0 represent the shrinkage of sample height and the original height of the sample before deformation, respectively. The use of pulsed direct current may generate spark discharges between the powder particles and plasma generation may also occur. Although the generation of a plasma has not been confirmed yet by direct experiment, it is likely that the electric field generates internal localized heating, impact pressure, and ionization, which promote mass transfer and accelerate localized reactions, and as a result lead to enhanced densification. It should be pointed out that a discharge process can play a major role only in the initial part of a sintering process but the other electrical field effects are operative over the entire sintering cycle, the reason being that the discharge process cannot be operative in fully dense samples. The field-enhanced mass transfer effects such as grain-boundary diffusion and grain-boundary migration processes can be effective in dense materials. In order to fully take advantage of these effects, we prepared partially dense materials instead of fully dense materials for subsequent superplastic deformation to enable both the discharge process and possible spark plasma effect to the whole deformation process. Here, we demonstrate spark-plasma-sintering, enhanced low temperature superplasticity in partially dense nanoceramic composites. The materials have nano-sized grains with a bimodal microstructure containing a certain amount of porosity. It is expected that these open porosities not only limit static grain growth but also may be effective second phase barriers to dynamic grain growth. In terms of these combined effects, it may be easily understood why such high deformation temperatures were observed in Shen's work since the only electrical field effect could be operative for the fully dense materials during the deformation. Figs. 6a and 6b show the spark-plasma-enhanced superplastically formed samples at 1000 and 1050 °C, respectively. It can be seen that the strain rates up to 10^{-2}/s could be achieved.

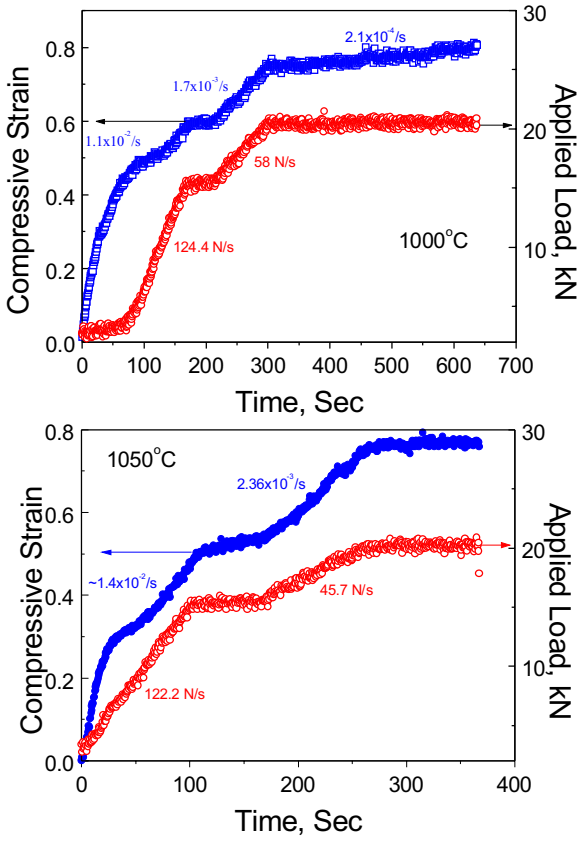

Fig. 6. Spark-plasma-enhanced superplastic deformation behavior of 50 vol.% $Al_2O_3/MgAl_2O_4$ composite. The compressive strain data obtained plotted vs. time for the composite at 1000 °C (a) and at 1050 °C (b).

A compressive strain of -0.8, equivalent to a reduction to half the original height, can be achieved without cracking. Surprisingly, the process deformation temperature is as low as 1000 °C – remarkably lower than those found for conventional superplastic ceramics. These record temperatures are comparable to that of Ni-based superalloys (typically, 950 °C), suggesting that an existing metallic superplastic shape tooling might be applied to nanoceramic composites. Importantly, the present study demonstrated that the more practical use of ceramic superplasticity is not in the shaping of already-dense materials but in the near net shape of dense parts from less-than-fully dense preforms. It should be noted that the same composites did not exhibit superplasticity by conventional deformation methods since both static grain growth during the slow heating and dynamic grain growth during high temperature deformation occur.

It is generally accepted that application of mechanical pressure is helpful in removing pores from compacts and enhancing diffusion. The increasing applied pressure during deformation is expected to provide extra strain energy to promote rapid densification and grain boundary sliding. Therefore, applying a high pressure at low temperature that allows the grain-boundary sliding to become kinetically favorable can enhance deformation rates. This is consistent with our findings where the strain rate increases with increasing loading rate. When a constant load instead of a constant stress is applied, the strain rates are significantly decreased. The latter is similar to the observations of Shen *et al.*'s work where they applied a constant load during the deformation, indicating a decreasing applied stress. It can also be noted that the strain rates are significantly increased when a little higher deformation temperature is applied (Fig. 6b) even though the loading rates are slightly lower, suggesting the temperature has profound effect on deformation.

Finally, it is very interesting to note that nearly nanosized microstructure has been obtained in the deformed composites whereas much grain growth can be seen in the non-deformed samples even at the same SPS temperature. These results suggest that SPS approach may be a new way for fabricating truly nanocrystalline ceramic composites with novel properties. Moreover, nearly fully dense materials can be achieved in the final products through SPS superplastic deformation. Interestingly, the deformed nanoceramic composites exhibit excellent infrared transparency (Fig. 7). To the best of our knowledge, infrared transparent nanoceramic composites instead of polycrystalline monolithic ceramic materials have never been reported in the literature. Such materials are highly desirable and have potential applications [12]. In conclusion, this new SPS approach, starting with partially dense materials and concurrent deformation and densification in the SPS apparatus, provides a new route for low temperature & high-strain-rate superplasticity for nanostructured materials and should impact and interest a broad range of scientists in materials research and superplastic forming technology.

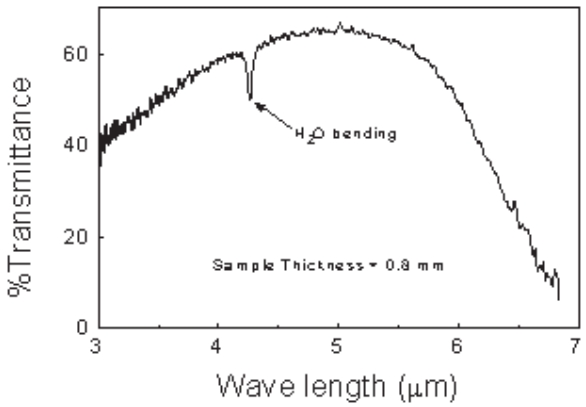

Fig. 7. Infrared spectrum of spark-plasma-enhanced superplastic formed sample at 1050 °C. The infrared spectra of the alumina-spinel composite samples were collected on a FTIR instrument (Mattson Galaxy Series FTIR 3000). The spectrometer was set to collect 16 scans in transmittance mode with a resolution of 4 cm^{-1} over a range from 650 nm to 16 μm. Over 40% transmittances have been obtained in the wavelength range of 3-6 μm, showing a maximum value of 65% at 5 μm. Note that there is an absorbing peak in the 4.4 mm due to the water bending effect that comes from environmental condition.

4. CONCLUSIONS

SPS technique has been found to not only be a very effective processing method for consolidation of composites containing carbon nanotubes with novel mechanical, electrical, thermal, and thermoelectric properties but also as a tooling for ultra-low-temperature superplasticity.

ACKNOWLEDGEMENTS

This investigation was supported in part by a grant (G-DAAD19-00-1-0185) from U.S. Army Research Office with Dr. William Mullins as the Program Man-

ager, a grant (N00014-03-1-0148) from Office of Naval Research with Dr. Lawrence Kabacoff as Program Manager, the HTML Proposal # 2003-025 by Oak Ridge National Laboratory, and the EMSL Proposal No. 3385 (2003) by Pacific Northwest National Laboratory.

REFERENCES

[1] R. H. Baughman, A. A. Zakhidov and W. A. de Heer // *Science* **297** (2002) 787.
[2] A. Peigney, Ch. Laurent, O. Dumortier and A. Rousset // *J. Euro. Ceram. Soc.* **18** (1998) 1995.
[3] R. W. Siegel, S. K. Chang, B. J. Ash, J. Stone, P. M. Ajayan, R. W. Doremus and L. S. Schadler // *Scripta Mater.* **44** (2001) 2061.
[4] G.-D. Zhan, J. D. Kuntz, J. Wan and A. K. Mukherjee // *Nature Mater*. **2** [1] (2003) 38.
[5] G.-D. Zhan, J. D. Kuntz, H. Wang, C.-M. Wang and A. K. Mukherjee // *Phil. Mag. Ltrs.* **84** (2004) 419.
[6] G.-D. Zhan, J. D. Kuntz, J. Garay and A. K. Mukherjee // *Appl. Phys. Lett.* **83** (2003) 1228.
[7] B. C. Sales // *Science* **295** (2002)1248.
[8] J. Hone, I. Ellwood, M. Muno, Ari Mizel, Marvin L. Cohen, A. Zettl, Andrew G. Rinzler and R. E. Smalley // *Phys. Rev. Lett*. **80** (1998) 1042.
[9] R. A. Hawsey, A. W. Murphy, W. S. Koncinski, *ORNL Superconducting Technology Program for Electrical Power Systems, Annual Report, FY 2001*, (published Feb. 2002) p. 45.
[10] Z. Shen, H. Peng and M. Nygren // *Adv. Mater.* **15** (2003) 1006.
[11] Z. Shen, H. Peng and M. Nygren // *J. Am. Ceram. Soc.* **87** (2004) 727.
[12] Daniel C. Harris, *Materials for Infrared Windows and Domes: Properties and Performance* (SPIE-the International Society for Optical Engineering, Bellingham, Washington, 1999).